Electron Transfer

DOI: 10.1002/anie.201206882

Self-Assembled Bilayer Films of Ruthenium(II)/Polypyridyl Complexes through Layer-by-Layer Deposition on Nanostructured Metal Oxides**

*Kenneth Hanson, Daniel A. Torelli, Aaron K. Vannucci, M. Kyle Brennaman, Hanlin Luo, Leila Alibabaei, Wenjing Song, Dennis L. Ashford, Michael R. Norris, Christopher R. K. Glasson, Javier J. Concepcion, and Thomas J. Meyer**

An increasingly important alternative to traditional silicon solar cells are low-cost dye-sensitized solar cells (DSSCs) and dye-sensitized photoelectrosynthesis cells (DSPECs). These devices utilize the attachment of multiple chromophores in DSSCs, or chromophores and catalysts in DSPECs, to the surfaces of nanostructured large-band-gap semiconducting metal oxides.[1,2] A number of strategies to assemble multiple small-molecule components on metal oxide films are being explored, including co-deposition[1,3] and preformed molecular assemblies.[4–11] These approaches suffer from inherent drawbacks, including decreased total light absorption by the chromophore and rapid back electron transfer for co-deposited films, and complex, multistep synthesis and low surface loadings (< 60 %) for preformed assemblies.[4,7]

We describe here a "layer-by-layer" approach for the assembly of multiple redox-active and/or chromophoric sites on nanocrystalline metal oxide surfaces by phosphonate/Zr^{IV} coordination linkages (Figure 1b). This strategy provides a simple, modular, and straightforward method for depositing functionalized dyes/catalysts on nanocrystalline oxide surfaces. It is an approach that has been exploited on planar surfaces by Mallouk and co-workers for multilayer alkyl diphosphonate films,[12,13] and by Haga and co-workers for multilayer Ru/polypyridyl assemblies.[14,15] As of yet, this self-assembly strategy has not been employed for the preparation of assemblies of chromophores and catalysts on nanostructured metal oxide substrates.

A family of phosphonate-derivatized $[Ru(bpy)_3]^{2+}$ chromophores was available for this study (bpy = 2,2′-bipyridine;

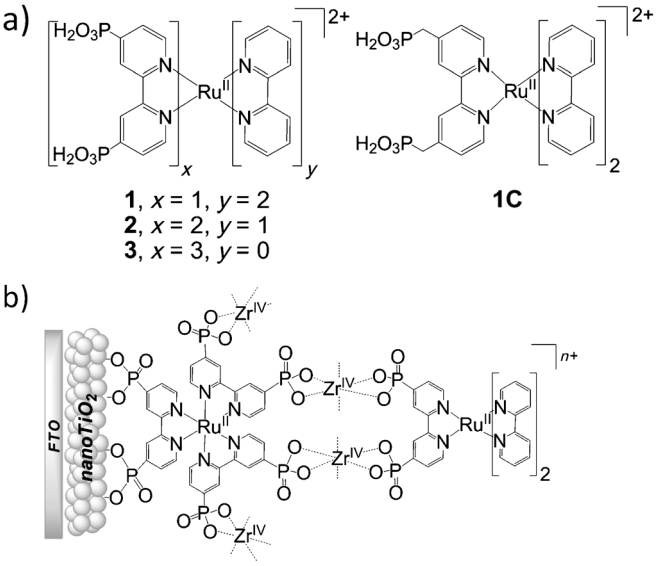

Figure 1. a) Structures of phosphonate-derivatized $[Ru(bpy)_3]^{2+}$ complexes **1**–**3** and **1C**. b) Schematic representation of the bilayer film assembly. FTO = fluorine-doped tin oxide.

Figure 1) with photophysical and electrochemical properties that have been characterized on nanocrystalline films of ZrO_2 and TiO_2.[16]

Bilayer structures were prepared by immersing nanocrystalline TiO_2 films in three separate aqueous solutions of $HClO_4$ (0.1 M) with 1) **3** (150 μM), 2) $ZrOCl_2$ (0.5 mM), and 3) **1**

[*] Dr. K. Hanson, D. A. Torelli, Dr. A. K. Vannucci, Dr. M. K. Brennaman, H. Luo, Dr. L. Alibabaei, Dr. W. Song, D. L. Ashford, M. R. Norris, Dr. C. R. K. Glasson, Dr. J. J. Concepcion, Prof. T. J. Meyer
Department of Chemistry
University of North Carolina at Chapel Hill
Chapel Hill, NC 27599 (USA)
E-mail: tjmeyer@unc.edu

[**] This work was partially funded by the UNC Energy Frontier Research Center (EFRC) "Center for Solar Fuels", an EFRC funded by the U.S. Department of Energy, Office of Science, Office of Basic Energy Sciences under award DE-SC0001011, which supported D.L.A., M.R.N. (M.K.B., J.J.C., T.J.M.), and electrochemical studies by K.H. (T.J.M.). The CCHF, an EFRC funded by the U.S. Department of Energy, Office of Science, Office of Basic Energy Sciences under award number DE-SC0001298 at the University of Virginia supported C.R.K.G. and W.S. (T.J.M.). Funding for the photophysical studies by K.H. (T.J.M.) was provided by the U.S. Department of Energy under award number DE-FG02-06ER15788. A.K.V. (T.J.M.) was supported by the Army Research Office Grant W911NF-09-1-0426. Support for L.A. (T.J.M.) was provided by Research Triangle Solar Fuels Institute. H.L. (T.J.M.) is supported by a Royster Society Fellowship. D.A.T. (T.J.M.) is an unfunded, undergraduate research student. We acknowledge support for the purchase of instrumentation from the UNC EFRC (Center for Solar Fuels), funded by the U.S. Department of Energy, Office of Science, Office of Basic Energy Sciences under award number DE-SC0001011), and UNC SERC ("Solar Energy Research Center Instrumentation Facility" funded by the U.S. Department of Energy Office of Energy Efficiency & Renewable Energy under award number DE-EE0003188).

Supporting information for this article (including steady-state absorption and emission spectra, time-resolved absorption and emission traces, XPS spectra, adsorption isotherms, CV traces, and other data) is available on the WWW under http://dx.doi.org/10.1002/anie.201206882 or from the author.

(150 μM), respectively, in a stepwise manner (≈12 h each). Absorption spectra of the films at each step of the loading procedure are shown in Figure 2. The total absorbance of TiO_2-(**3**)-Zr-(**1**) is approximately twice that of the monolayer film (TiO_2-(**3**)), consistent with a ratio for **3** to **1** of approximately 1:1.

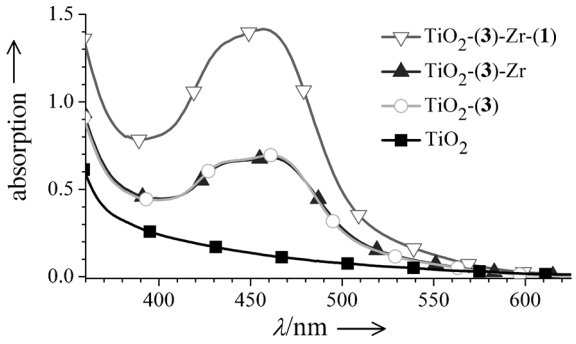

Figure 2. Absorption spectra of dry films (4 μm TiO_2).

When TiO_2-(**3**) is immersed in a solution of **1** but not treated with $ZrOCl_2$, no spectral change was observed. This result is consistent with a closely packed monolayer of **3**, which inhibits surface binding of **1**.

Surface modifications that accompany the treatment of TiO_2-(**3**) with $ZrOCl_2$ were investigated by attenuated total reflectance infrared spectroscopy (ATR-IR). The disappearance of the symmetric stretching band of the non-surface-bound P–OH group[17] at 935 cm^{-1} and the appearance of a higher energy band at 995 cm^{-1} is indicative of phosphonate coordination to Zr^{IV} (Figure S1 in the Supporting Information).[18,19] Coordination of Zr^{IV} was complete in less than 20 minutes (Figure S2).

X-ray photoelectron spectroscopy (XPS) of the TiO_2-(**3**)-Zr films showed a Zr to Ru ratio of about 4:1. This ratio is consistent with the coordination of Zr^{IV} to four non-surface-bound PO_3H_2 groups in **3** (Figure 1) with the interfacial stoichiometry of (**3**)-$(Zr^{IV})_4$.

The coordination of Zr^{IV} ions to ZrO_2-(**3**) and TiO_2-(**3**) has a minimal effect on photophysical and electrochemical properties of the films (results summarized in the Supporting Information). Addition of **1** to TiO_2-(**3**)-Zr films follows Langmuir isotherm behavior (Figure S8) with a maximum surface coverage (3.0×10^{-8} mol cm^{-2} μm^{-1} for a 7 μm film) comparable to that of **1** directly bound to TiO_2 and the initial surface loading of **3**.[16] Zr^{IV} coordination is maintained during the loading of **1**, as shown by XPS measurements of the Zr/Ru ratio (Figure S10).

These results are all consistent with formation of a (**3**)-$(Zr^{IV})_4$-(**1**) bilayer structure on TiO_2 (herein simplified to TiO_2-(**3**)-Zr-(**1**)), with the complexes linked by Zr^{IV} coordination. This bilayer architecture maintains a maximum surface coverage for both chromophores and effectively doubles the number of chromophores per unit surface area. The local coordination chemistry and structure for TiO_2-(**3**)-Zr-(**1**) are unknown. We have no direct information about the nature of the binding of outer chromophore **1** or even of the number of Zr sites involved. The schematic representation shown in Figure 1b is reasonable but unsupported. The results of a preliminary molecular modeling study suggest that the bonding motif shown in Figure 1b is possible, but do not exclude other bonding modes.

The photophysical properties of the bilayer film were investigated on ZrO_2, which is inert toward electron injection from the lowest-lying metal-to-ligand charge-transfer (MLCT) excited states of both **1** and **3**. For ZrO_2-(**3**)-Zr-(**1**), steady-state emission spectra in 0.1 M $HClO_4$ closely resemble the spectrum of ZrO_2-(**1**) (Figure 3) with λ_{max}(emission) = 665 nm compared to 645 nm for ZrO_2-(**3**)-Zr.

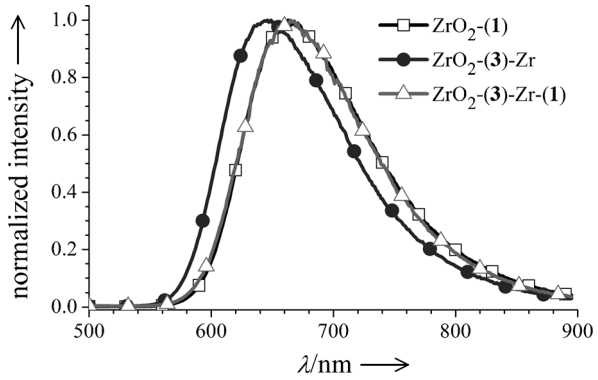

Figure 3. Room-temperature emission spectra in aqueous solution of $HClO_4$ (0.1 M; Ex: 450 nm).

Because **1** and **3** are excited equally at 450 nm, the observation of emission from ZrO_2-(**3**)-Zr-(**1**) is consistent with both direct excitation of **1** and "inside-to-outside" intra-assembly energy transfer (**3** to **1**), which is favored by approximately 465 cm^{-1}. From the results of time-resolved emission measurements, intra-assembly energy transfer is rapid, occurring in less than 200 ns (Figure S13).

The direction of the energy transfer was reversed by using **1C** (λ_{max} = 630 nm; Figure 1a) in the external site. In this configuration, ZrO_2-(**3**)-Zr-(**1C**), "outside-to-inside" energy transfer is favored by approximately 370 cm^{-1}. Both steady-state and time-resolved emission measurements (Figure S12 and S13) for ZrO_2-(**3**)-Zr-(**1C**) indicate that energy transfer occurs from **1C** toward the interface to **3**. This result is important because it shows that manipulation of components can be used to achieve an "antenna effect" with the absorbed energy directed to the interface. As found for other dynamic processes on nanocrystalline metal oxide interfaces, emission decay kinetics for the surface assemblies are highly non-exponential. A complete analysis of intra-assembly dynamics in ZrO_2-(**3**)-Zr-(**1**) and ZrO_2-(**3**)-Zr-**1C**) will be reported elsewhere.

The results of long-term photolysis studies show that both TiO_2-(**3**)-Zr-(**1**) and TiO_2-(**3**)-Zr-(**1C**) have interfacial photostabilities ($k_{des} = 6.6\times10^{-5}$ s^{-1} and 6.4×10^{-5} s^{-1}; k_{des} is the rate constant for desorption) comparable to the component monolayer films ($k_{des} = 3.5$–5.8×10^{-5} s^{-1}).[20]

Two 4,4′-$(PO_3H_2)_2$bpy ligands on the inside chromophore are sufficient for bilayer formation. The adsorption isotherm

for **1** on TiO_2-(**2**)-Zr (Figure S16), to give TiO_2-(**2**)-Zr-(**1**), has a maximum surface loading (3.4×10^{-8} mol cm^{-2} μm^{-1}) comparable to the monolayer films of **2** and **1**. Formation of bilayer films can also be achieved with $(COOH)_2$bpy-derivatized complexes, as shown for the DSSC dyes **N719** and **RuC** (Figure 4). Absorption spectra of the interfacial assemblies TiO_2-(**2**)-Zr-(**N719**) and TiO_2-(**N719**)-(Zr)-(**RuC**), are the approximate sum of the component monolayer films (Figure S17).

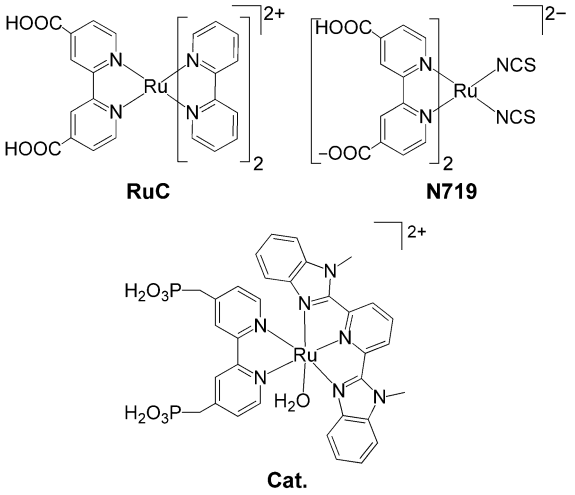

Figure 4. Structure of **RuC**, **N719**, and **Cat**.

Attempts to form the "inverse" TiO_2-(**N719**)-Zr-(**1**) assembly with surface-bound carboxylates and external phosphonates were unsuccessful. Initial loading of **N719** followed by treatment with $ZrOCl_2$ and addition of **1** results in a decrease in absorption for **N719** (Figure S18c). This behavior is presumably a consequence of the higher binding affinity of phosphonate groups on TiO_2 compared to carboxylates. This affinity leads to partial exchange of carboxylate-bound **N719** for phosphonate-bound **1** and loss of **N719** from the surface.[20]

An important element in the design of photoanodes in DSPECs is the assembly of chromophores and water oxidation catalysts on TiO_2 or other large-band-gap metal oxides. The absorption spectrum of a TiO_2 film after stepwise loading of **2** and $ZrOCl_2$ followed by the water oxidation catalyst $[Ru(4,4'\text{-}(CH_2PO_3H_2)_2bpy)(Mebimpy)(H_2O)]^{2+}$ (**Cat**, Mebimpy = 2,6-bis(1-methylbenzimidazol-2-yl)pyridine; Figure 4) is the sum of the monolayer spectra (Figure S18d).[21] This observation is important as it opens the door to a general, straightforward strategy for creating chromophore–catalyst assemblies. Cyclic voltammetry and steady-state current measurements of **Cat** and (**2**)-Zr-(**Cat**) on nanocrystalline indium tin oxide (nanoITO) films[21] in aqueous solution of $HClO_4$ (0.1 M) show that the chromophore–catalyst bilayer maintains the electrocatalytic current response exhibited by the catalyst alone (Figures S18 and S19). With long-term electrolysis of the nanoITO-(**2**)-Zr-(**Cat**) bilayer film at 1.7 V versus NHE (Figure S20), a catalytic current was maintained over a period of several hours. GC analysis supports the formation of O_2 as the product (Figure S21).

Dynamics of interfacial electron transfer in the layer-by-layer chromophore–catalyst assembly were investigated by nanosecond transient absorption measurements in aqueous solution of $HClO_4$ (0.1 M). Transient absorption difference spectra for TiO_2-(**2**)-Zr, TiO_2-(**Cat**) and TiO_2-(**2**)-Zr-(**Cat**) were acquired approximately 10 ns after 532 nm excitation (Figure 5 a).

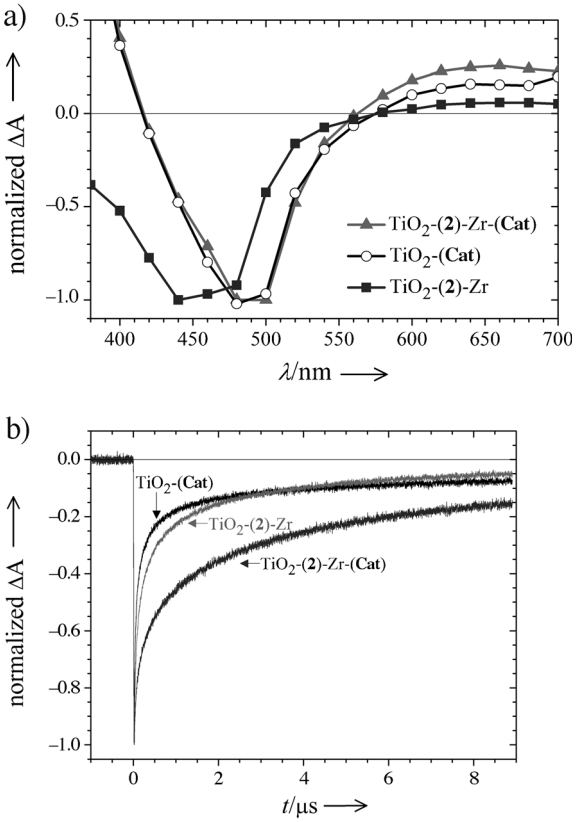

Figure 5. Transient absorption difference spectra acquired 10 ns after laser flash excitation (a) and absorption-time traces at 490 nm (b) for TiO_2-(**2**)-Zr, TiO_2-(**Cat**), and TiO_2-(**2**)-Zr-(**Cat**) in aqueous solution of $HClO_4$ (0.1 M; Ex: 532 nm).

The ground-state MLCT bleaches at around 460 nm for TiO_2-(**2**)-Zr and at around 490 nm for TiO_2-(**Cat**), are expected for singly oxidized **2** (**2**$^+$) and **Cat** (**Cat**$^+$) following excited-state electron injection [Eq. (1) and (2)].[16,21]

$$TiO_2\text{-}(\mathbf{2})\text{-}Zr \xrightarrow{h\nu} TiO_2(e^-)\text{-}(\mathbf{2}^+)\text{-}Zr \quad (1)$$

$$TiO_2\text{-}(\mathbf{Cat}) \xrightarrow{h\nu} TiO_2(e^-)\text{-}(\mathbf{Cat}^+) \quad (2)$$

The characteristic bleach at around 490 nm for **Cat**$^+$ is evident in the transient absorption spectrum of the assembly TiO_2-(**2**)-Zr-(**Cat**). This observation is consistent with photoexcitation of **2** [Eq. (3)], electron injection into TiO_2 [Eq. (4)], and "inside-to-outside" electron transfer [Eq. (5)]. The reaction in Equation (5) is important as the first step in an overall water-oxidation cycle for **Cat** at the photoanode of

a DSPEC.

$$TiO_2\text{-}(2)\text{-}Zr\text{-}(\mathbf{Cat}) + h\nu \rightarrow TiO_2\text{-}(2^*)\text{-}Zr\text{-}(\mathbf{Cat}) \quad (3)$$

$$TiO_2\text{-}(2^*)\text{-}Zr\text{-}(\mathbf{Cat}) \rightarrow TiO_2(e^-)\text{-}(2^+)\text{-}Zr\text{-}(\mathbf{Cat}) \quad (4)$$

$$TiO_2(e^-)\text{-}(2^+)\text{-}Zr\text{-}(\mathbf{Cat}) \rightarrow TiO_2(e^-)\text{-}(2)\text{-}Zr\text{-}(\mathbf{Cat}^+) \quad (5)$$

There may also be a contribution to the appearance of $\mathbf{Cat}^+$ by direct light absorption and remote electron injection by $\mathbf{Cat}^*$. This contribution is expected to be small, given the short excited-state lifetime (< 10 ns) and the relatively large separation distance of $\mathbf{Cat}^*$ from the oxide surface. In its Ru^{II} form, the catalyst acts largely as a nonproductive light absorber [Eq. (6)].

$$TiO_2\text{-}(2)\text{-}Zr\text{-}(\mathbf{Cat}) + h\nu \rightarrow TiO_2\text{-}(2)\text{-}Zr\text{-}(\mathbf{Cat}^*) \rightarrow TiO_2\text{-}(2)\text{-}Zr\text{-}(\mathbf{Cat}) \quad (6)$$

Back electron transfer from $TiO_2(e^-)$ to $(\mathbf{Cat}^+)$, $(\mathbf{2}^+)$-Zr, and $(\mathbf{2})$-Zr-$(\mathbf{Cat}^+)$ was monitored at 490 nm (Figure 5b). As commonly found for back-electron-transfer dynamics at TiO_2 interfaces, the kinetics are complex but can be characterized by the time it takes for half the total absorbance change to occur ($t_{1/2}$). These values increase in the order: $TiO_2(e^-)$-$(\mathbf{Cat}^+)$ (80 ns) < $TiO_2(e^-)$-$(\mathbf{2}^+)$-Zr (165 ns) < $TiO_2(e^-)$-$(\mathbf{2})$-$(\mathbf{Zr})$-$(\mathbf{Cat}^+)$ (755 ns). The order of magnitude decrease in $t_{1/2}$ between $TiO_2(e^-)$-$(\mathbf{Cat}^+)$ and $TiO_2(e^-)$-$(\mathbf{2})$-Zr-$(\mathbf{Cat}^+)$, demonstrates a significant slowing of electron transfer as a result of the spatial separation between $TiO_2(e^-)$ and $\mathbf{Cat}^+$. A complete investigation of the electron-transfer dynamics in $TiO_2(e^-)$-$(\mathbf{2})$-Zr-$(\mathbf{Cat}^+)$ is currently underway.

In conclusion, we have demonstrated the feasibility of a layer-by-layer strategy for spontaneously assembling chromophore–chromophore and chromophore–catalyst arrays on nanocrystalline metal oxide films. The strategy is general and offers considerable flexibility based on phosphonate- or carboxylate-binding groups with Zr^{IV} as bridging ions. The resulting structures are capable of supporting rapid intralayer energy and electron transfer. The assembly procedure and associated energy/electron-transfer characteristics are an important first step toward new device architectures based on molecular bilayers on mesoscopic films. We are extending the initial observations in both DSSC and DSPEC applications.

Received: August 24, 2012
Published online: November 9, 2012

Keywords: bilayers · chromophores · electron transfer · energy transfer · self-assembly

[1] A. Yella, H.-W. Lee, H. N. Tsao, C. Yi, A. K. Chandiran, M. K. Nazeeruddin, E. W.-G. Diau, C.-Y. Yeh, S. M. Zakeeruddin, M. Grätzel, *Science* **2011**, *334*, 629.
[2] G. F. Moore, J. D. Blakemore, R. L. Milot, J. F. Hull, H.-e. Song, L. Cai, C. A. Schmuttenmaer, R. H. Crabtree, G. W. Brudvig, *Energy Environ. Sci.* **2011**, *4*, 2389.
[3] S. Ardo, G. J. Meyer, *J. Am. Chem. Soc.* **2010**, *132*, 9283.
[4] T. Rawling, C. Austin, F. Buchholz, S. B. Colbran, A. M. McDonagh, *Inorg. Chem.* **2009**, *48*, 3215.
[5] W. Song, C. R. K. Glasson, H. Luo, K. Hanson, M. K. Brennaman, J. J. Concepcion, T. J. Meyer, *J. Phys. Chem. Lett.* **2011**, *2*, 1808.
[6] A. C. Lees, C. J. Kleverlaan, C. A. Bignozzi, J. G. Vos, *Inorg. Chem.* **2001**, *40*, 5343.
[7] C. J. Kleverlaan, M. T. Indelli, C. A. Bignozzi, L. Pavanin, F. Scandola, G. M. Hasselman, G. J. Meyer, *J. Am. Chem. Soc.* **2000**, *122*, 2840.
[8] Y. Lee, S.-R. Jang, R. Vittal, K.-J. Kim, *New J. Chem.* **2007**, *31*, 0.
[9] R. Argazzi, C. A. Bignozzi, T. A. Heimer, G. J. Meyer, *Inorg. Chem.* **1997**, *36*, 2.
[10] C. Kleverlaan, M. Alebbi, R. Argazzi, C. A. Bignozzi, G. M. Hasselmann, G. J. Meyer, *Inorg. Chem.* **2000**, *39*, 1342.
[11] S. H. Wadman, Y. M. van Leeuwen, R. W. A. Havenith, G. P. M. van Klink, G. van Koten, *Organometallics* **2010**, *29*, 5635.
[12] H. Lee, L. J. Kepley, H. G. Hong, S. Akhter, T. E. Mallouk, *J. Phys. Chem.* **1988**, *92*, 2597.
[13] H. Lee, L. J. Kepley, H. G. Hong, T. E. Mallouk, *J. Am. Chem. Soc.* **1988**, *110*, 618.
[14] T. Ishida, K.-i. Terada, K. Hasegawa, H. Kuwahata, K. Kusama, R. Sato, M. Nakano, Y. Naitoh, M.-a. Haga, *Appl. Surf. Sci.* **2009**, *255*, 8824.
[15] K. Terada, K. Kobayashi, J. Hikita, M.-a. Haga, *Chem. Lett.* **2009**, *38*, 416.
[16] K. Hanson, M. K. Brennaman, A. Ito, H. Luo, W. Song, K. A. Parker, R. Ghosh, M. R. Norris, C. R. K. Glasson, J. J. Concepcion, R. Lopez, T. J. Meyer, *J. Phys. Chem. C* **2012**, *116*, 14837.
[17] T. Undabeytia, E. Morillo, C. Maqueda, *J. Agric. Food Chem.* **2002**, *50*, 1918.
[18] W. Gao, L. Dickinson, C. Grozinger, F. G. Morin, L. Reven, *Langmuir* **1996**, *12*, 6429.
[19] P. Wang, C. Klein, J.-E. Moser, R. Humphry-Baker, N.-L. Cevey-Ha, R. Charvet, P. Comte, S. M. Zakeeruddin, M. Grätzel, *J. Phys. Chem. B* **2004**, *108*, 17553.
[20] K. Hanson, M. K. Brennaman, H. Luo, C. R. K. Glasson, J. J. Concepcion, W. Song, T. J. Meyer, *ACS Appl. Mater. Interfaces* **2012**, *4*, 1462.
[21] Z. Chen, J. J. Concepcion, J. F. Hull, P. G. Hoertz, T. J. Meyer, *Dalton Trans.* **2010**, *39*, 6950.

